

## Supplementary Information

**From fluorene molecules to ultrathin carbon nanonets with enhanced charge transfer capability for supercapacitors**

Xiaojun He<sup>a,\*</sup>, Xiaoyu Xie<sup>a</sup>, Jingxian Wang<sup>a</sup>, Xiufang Ma<sup>b</sup>, Yuanyang Xie<sup>a</sup>, Jing Gu<sup>a</sup>, Nan Xiao<sup>c</sup>, Jieshan Qiu<sup>d,\*</sup>

## Figure captions

**Figure S1.** (a) TEM image of sheet-like MgO particles. (b, c) Size of MgO particles.

**Figure S2.** TEM images of (a, b) UCN<sup>0</sup><sub>0-10</sub>. UCN<sup>0</sup><sub>0-10</sub> is made on 2 g naked nano-MgO particles in another corundum boat.

**Figure S3.** Schematic for the relative position of corundum boats in horizontal tubular furnace.

**Figure S4.** N<sub>2</sub> adsorption-desorption isotherms of: (a) UCN<sub>0-10</sub>, (c) UCN<sub>3-0</sub>. Pore size distribution curves of: (b) UCN<sub>0-10</sub>, (d) UCN<sub>3-0</sub>. (e) XRD patterns of UCN<sub>0-10</sub> and UCN<sub>2-10</sub>. (f) Raman spectra of UCN<sub>0-10</sub> and UCN<sub>2-10</sub>.

**Figure S5.** Carbon nanonets from fluorene molecules via step-by-step self-assembly process.

**Figure S6.** Schematic for the step-by-step assembly of six-membered fluorene rings.

**Figure S7.** Schematic for the assembly of UCN from fluorene molecules.

**Figure S8.** Schematic for the assembly of UCNs from fluorene molecules in nano-MgO-template-confinement space with the aid of KOH.

**Figure S9.** (a) CV curves of UCN<sub>3-10</sub> electrode at 2 and 5 mV s<sup>-1</sup>. (b) CV curves of UCN<sub>0-10</sub> electrode at 2 and 5 mV s<sup>-1</sup>.

## Table captions

**Table S1** The pore structure parameters of UCN samples.

**Table S2** The XPS results of the UCN samples.

**Table S3** Comparison of the specific capacitance of the UCN electrode with that of the hollow nanostructure carbons.

**Table S4** Comparison of the performance of the UCN electrode with that of the carbon-based electrode materials.

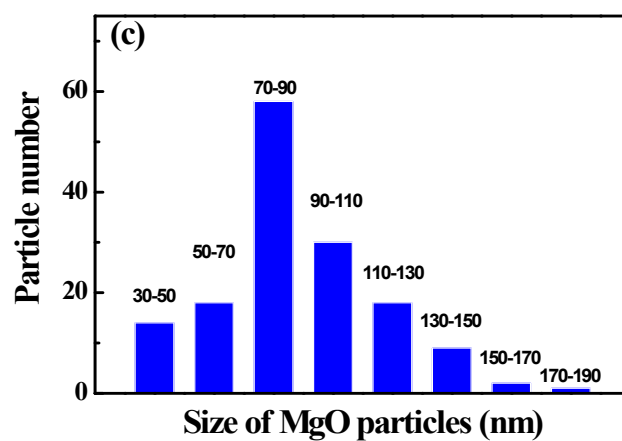
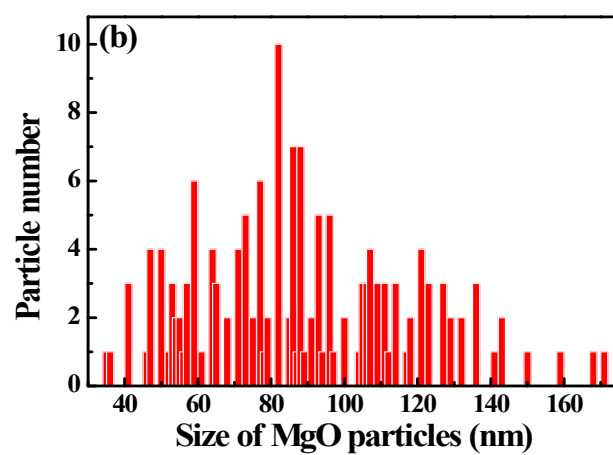
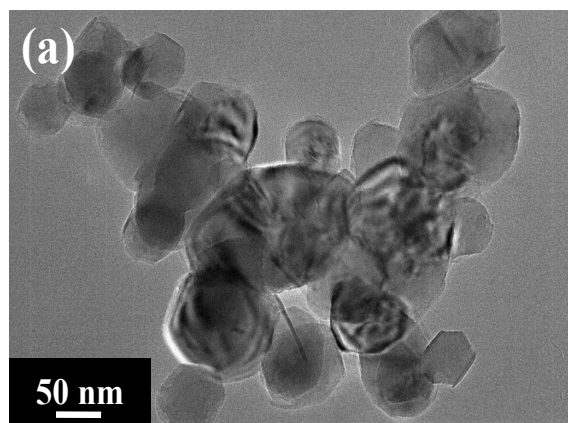


**Figure S1.** (a) TEM image of sheet-like MgO particles. (b, c) Size of MgO particles.

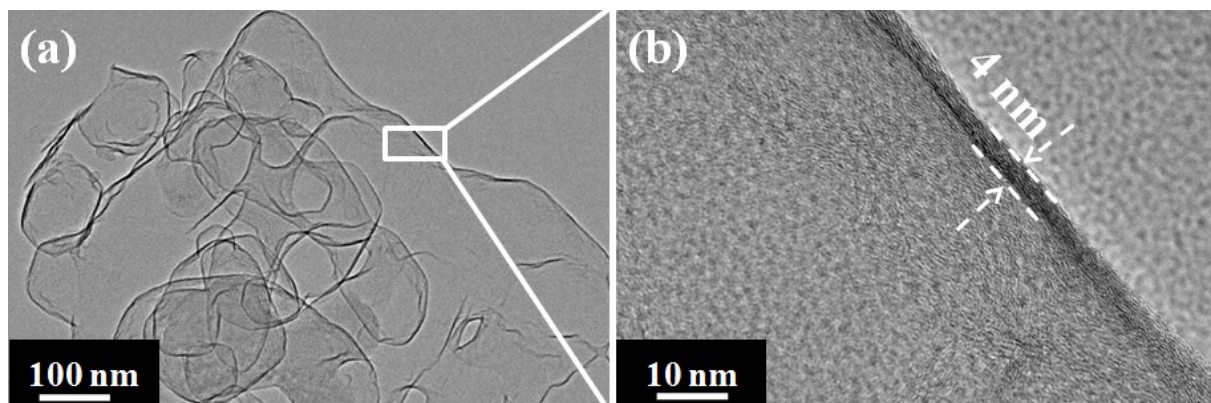


**Figure S2.** TEM images of (a, b)  $UCN^{0-10}$ .  $UCN^{0-10}$  is made on 2 g naked nano-MgO particles in another corundum boat.

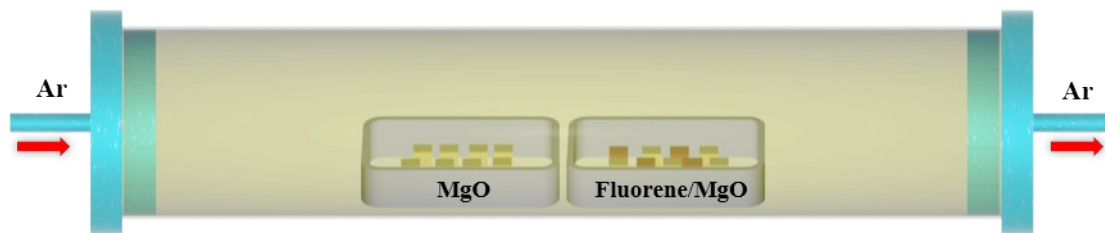


**Figure S3.** Schematic for the relative position of corundum boats in horizontal tubular furnace.

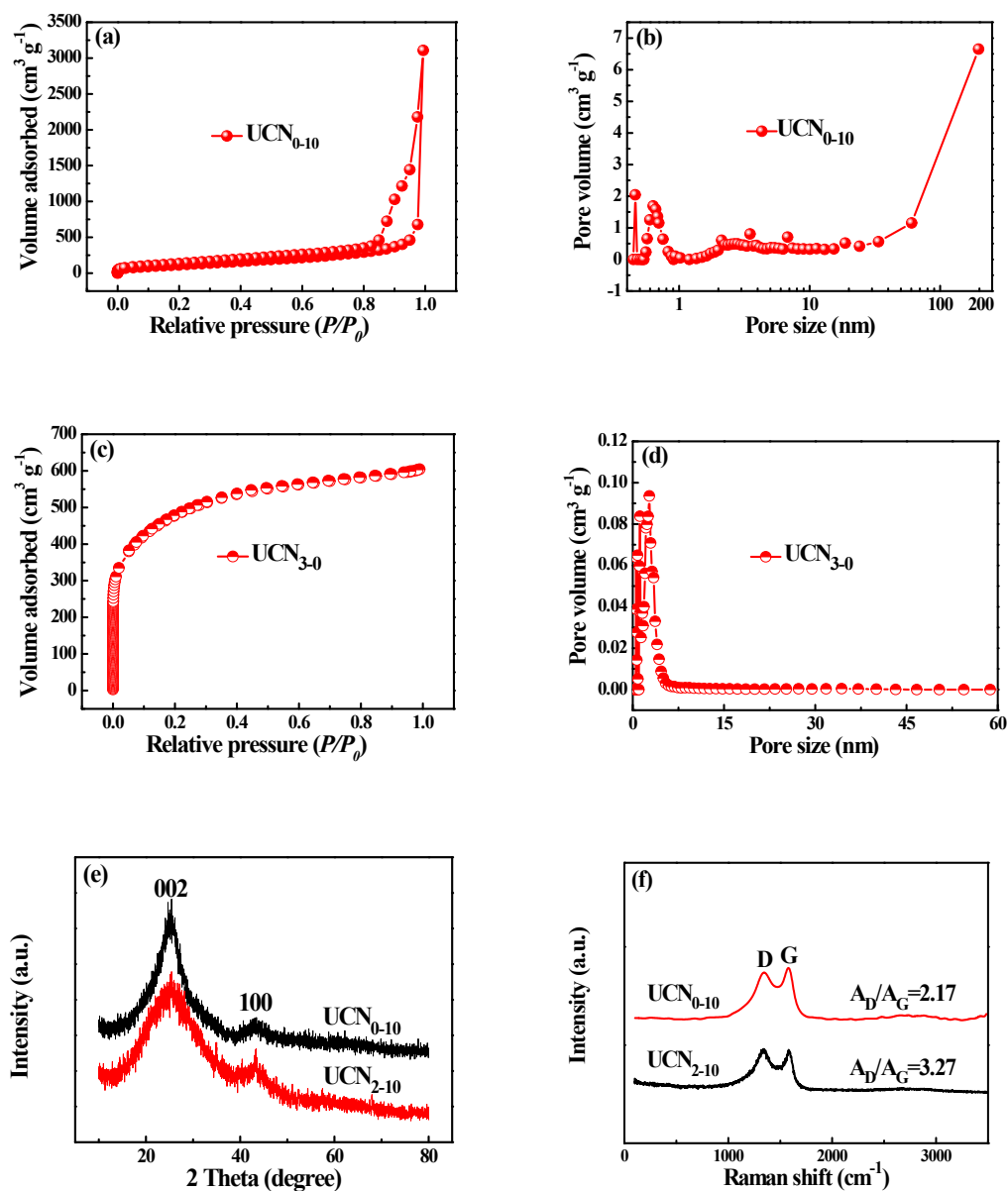


**Figure S4.** N<sub>2</sub> adsorption-desorption isotherms of: (a) UCN<sub>0-10</sub>, (c) UCN<sub>3-0</sub>. Pore size distribution curves of: (b) UCN<sub>0-10</sub>, (d) UCN<sub>3-0</sub>. (e) XRD patterns of UCN<sub>0-10</sub> and UCN<sub>2-10</sub>. (f) Raman spectra of UCN<sub>0-10</sub> and UCN<sub>2-10</sub>.

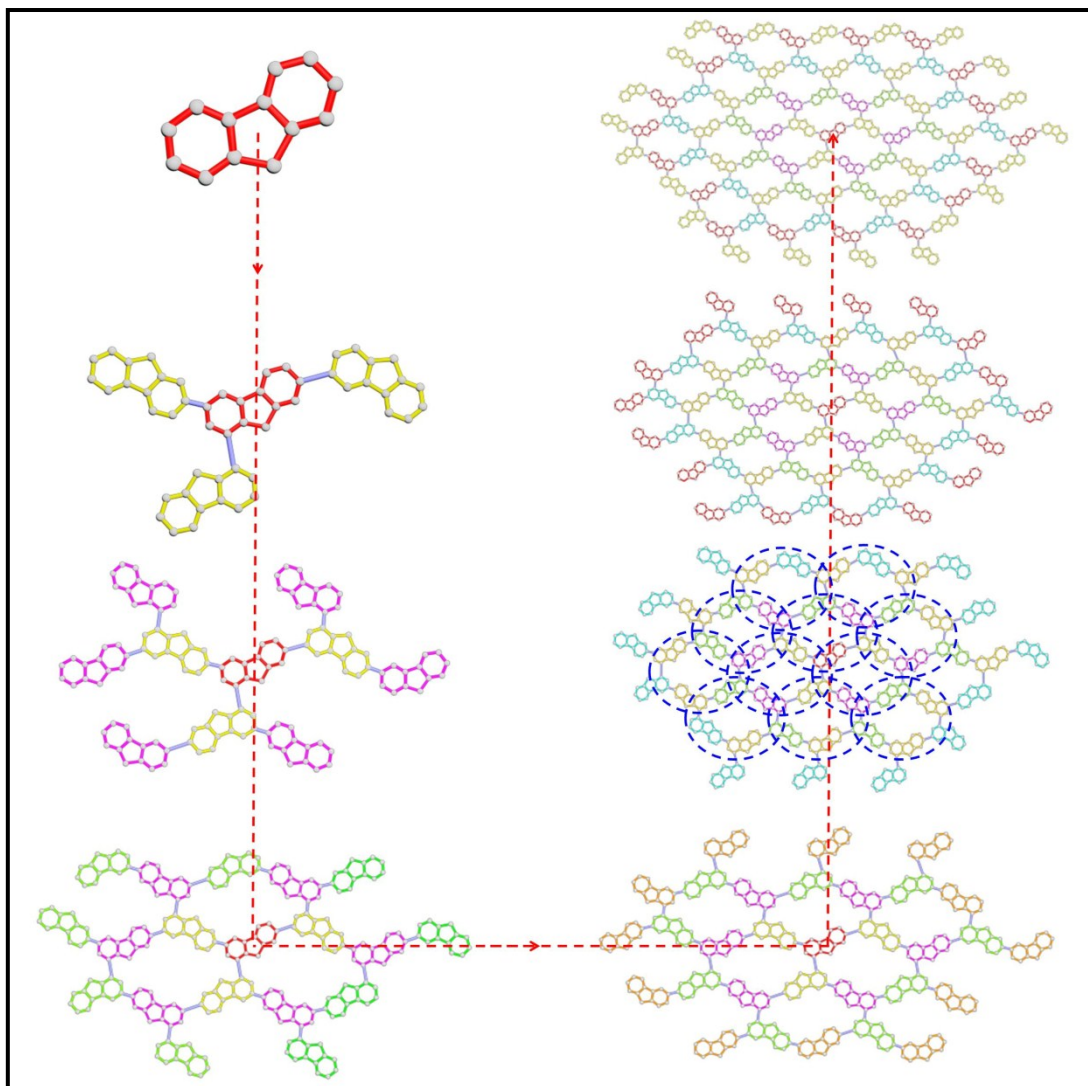


**Figure S5.** Carbon nanonets from fluorene molecules via step-by-step self-assembly process.

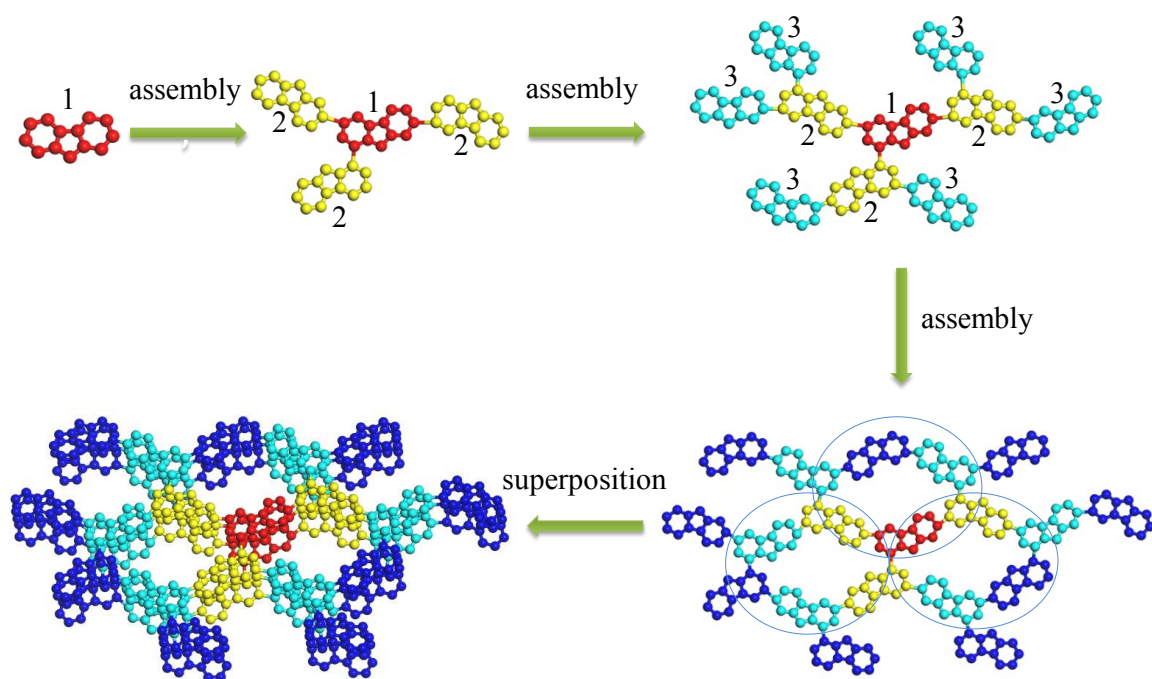


**Figure S6.** Schematic for the step-by-step assembly of six-membered fluorene rings.

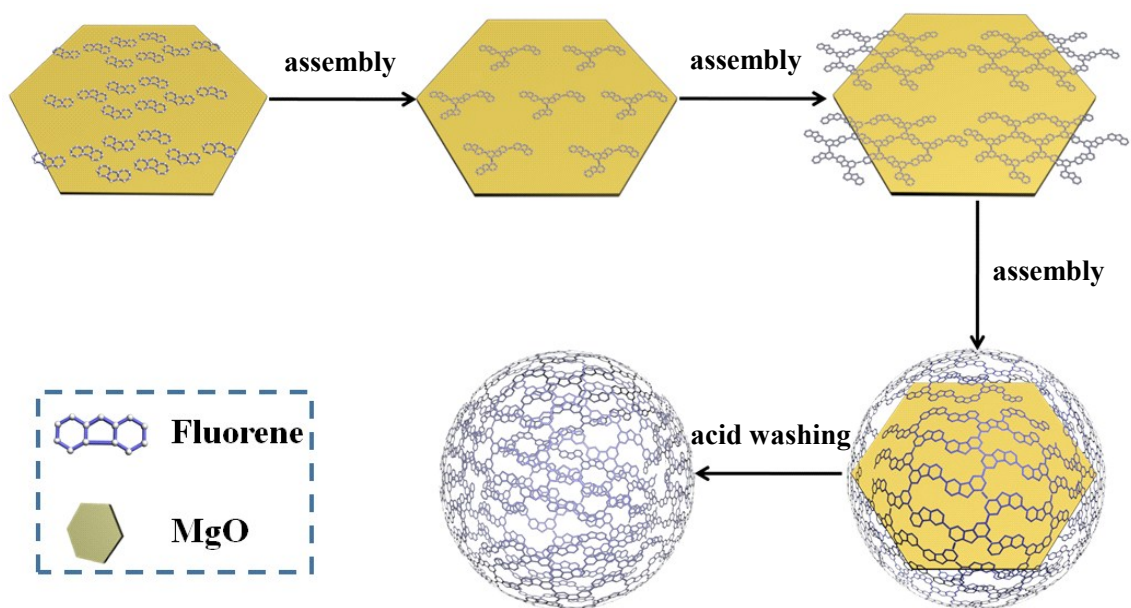


**Figure S7.** Schematic for the assembly of UCN from fluorene molecules.

**Table S1** The pore structure parameters of UCN samples.

<b>Samples</b>	<b>BET surface area (m<sup>2</sup> g<sup>-1</sup>)</b>	<b>Average pore diameter (nm)</b>	<b>Pore volume (cm<sup>3</sup> g<sup>-1</sup>)</b>	<b>Micropore volume (cm<sup>3</sup> g<sup>-1</sup>)</b>
UCN <sub>0-10</sub>	461	41.7	4.81	0.04
UCN <sub>2-10</sub>	2107	2.31	1.21	0.88
UCN <sub>3-10</sub>	2550	2.40	1.57	1.06
UCN <sub>4-10</sub>	1581	2.24	0.88	0.68
UCN <sub>3-0</sub>	1701	2.20	0.94	0.25

**Table S2** The XPS results of the UCN samples.

<b>Samples</b>	<b>C1s (%)</b>	<b>O1s (%)</b>	<b>O1s</b>		
			<b>C=O (%)</b>	<b>C-O (%)</b>	<b>O-H (%)</b>
UCN <sub>2-10</sub>	78.63	21.37	5.95	3.91	11.51
UCN <sub>3-10</sub>	89.52	10.48	5.35	5.13	0
UCN <sub>4-10</sub>	78.15	21.85	13.31	8.54	0

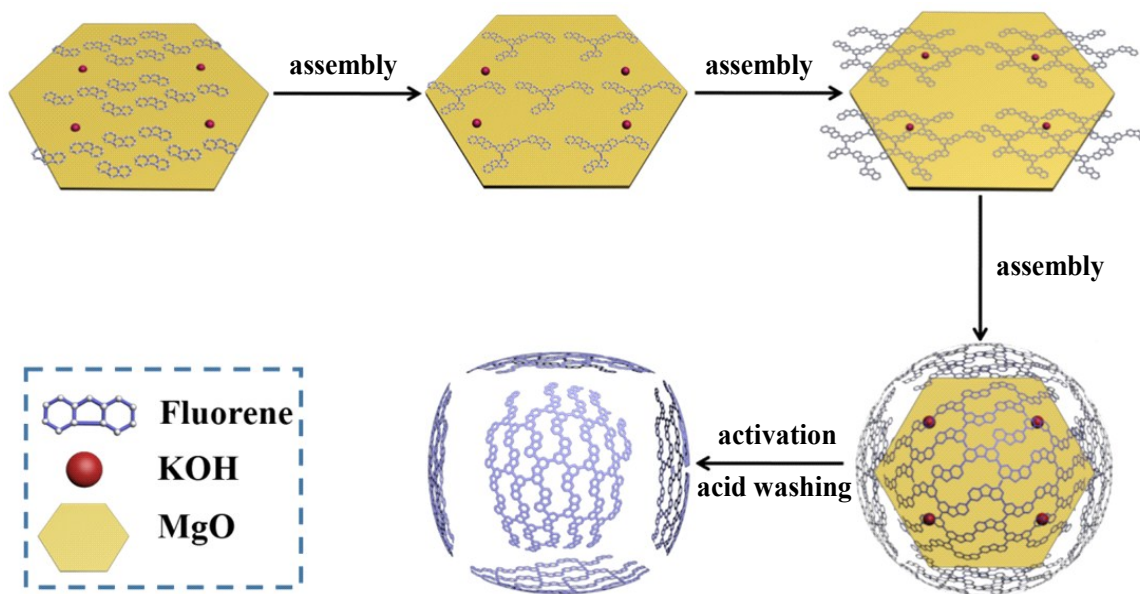


**Figure S8.** Schematic for the assembly of UCNs from fluorene molecules in nano-MgO-template-confinement space with the aid of KOH.

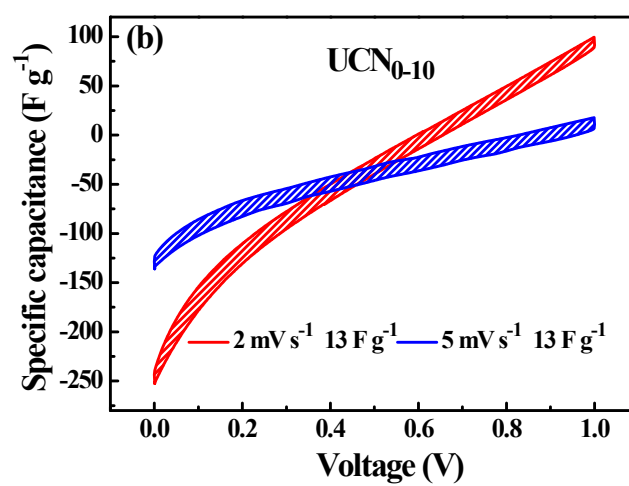
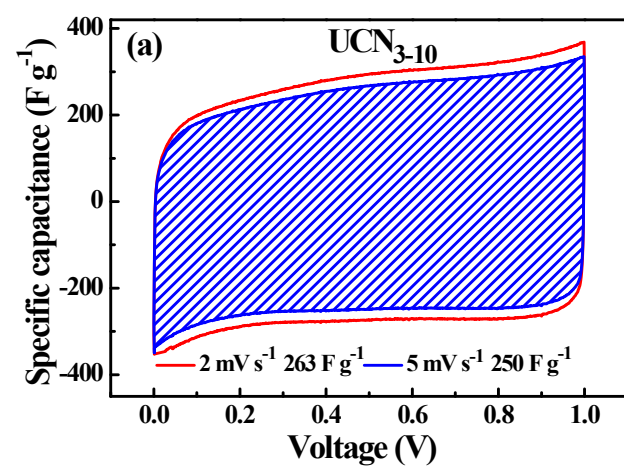


**Figure S9.** (a) CV curves of UCN<sub>3-10</sub> electrode at 2 and 5 mV s<sup>-1</sup>. (b) CV curves of UCN<sub>0-10</sub> electrode at 2 and 5 mV s<sup>-1</sup>.

**Table S3** Comparison of the specific capacitance of the UCN electrode with that of the hollow nanostructure carbons.

Materials	Electrolyte	Current density (A g <sup>-1</sup> )	Specific capacitance (F g <sup>-1</sup> )	Ref.
BFC	6 M KOH	1.0	200	1
CCNC1	6 M KOH	0.1	205	2
SRPC-4K-900	6 M KOH	0.5	276	3
HP-CF	6 M KOH	0.5	238	4
NPC-m	6 M KOH	0.5	301	5
HPCNC-700-a	6 M KOH	1.0	288	6
HPCNFs-N	6 M KOH	1.0	307	7
h-CNS900	6 M KOH	0.1	272	8
UCN <sub>3-10</sub>	6 M KOH	0.05	313	This work
		1.0	282	

**Table S4** Comparison of the performance of the UCN electrode with that of the carbon-based electrode materials.

Materials	$S_{\text{BET}}$ ( $\text{m}^2 \text{g}^{-1}$ )	Electrolyte	Current density ( $\text{A g}^{-1}$ )	$C_g$ ( $\text{F g}^{-1}$ )	Ref.
a-CBP	1326	6 M KOH	2 $\text{mV s}^{-1}$	296	9
FPGF-200	7	6 M KOH	0.5	388	10
N-ACN <sub>10</sub>	1630	6 M KOH	2 $\text{mV s}^{-1}$	331	11
TRGN	–	6 M KOH	2 $\text{mV s}^{-1}$	442.8	12
a-PNC-10	434	6 M KOH	2 $\text{mV s}^{-1}$	369	13
S-3DCN	575	6 M KOH	1.0	395	14
GSI/Ni	–	6 M KOH	0.2	236	15
WPCNS	1136	6 M KOH	0.05	286	16
UCN <sub>3-10</sub>	2550	6 M KOH	0.05 1.0	313 282	This work

## References

- 1 F. Sun, Z. B. Qu, J. H. Gao, H. B. Wu, F. Liu, R. Han, L. J. Wang, T. Pei, G. B. Zhao and Y. F. Lu, *Adv. Funct. Mater.* 2018, 28, 180419.
- 2 Y. F. Bu, T. Sun, Y. J. Cai, L. Y. Du, O. Zhuo, L. J. Yang, Q. Wu, X. Z. Wang and Z. Hu, *Adv. Mater.* 2017, 29, 1700470.
- 3 N. N. Guo, M. Li, Y. Wang, X. K. Sun, F. Wang and R. Yang, *ACS Appl. Mater. Interfaces*, 2016, 8, 33626–33634.
- 4 J. Z. Chen, J. L. Xu, S. Zhou, N. Zhao and C.-P. Wong, *Nano Energy*, 2016, 25, 193–202.
- 5 X. W. Dong, Z. Yang, X. Wu, Y. S. Luo, T. Q. Chen, M. Li, N. T. Hu and Y. F. Zhang, *Electrochim. Acta*, 2017, 251, 263–269.
- 6 J. Q. Shao, M. Y. Song, G. Wu, Y. H. Zhou, J. F. Wan, X. Ren and F. W. Ma, *Energy Storage Mater.* 2018, 13, 57–65.
- 7 L.-F. Chen, Y. Lu, L. Yu and X. W. Lou, *Energy Environ. Sci.*, 2017, 10, 1777–1783.
- 8 Q.-L. Zhu, P. Pachfule, P. Strubel, Z. P. Li, R. Q. Zou, Z. Liu, S. Kaskel and Q. Xu, *Energy Storage Mater.*, 2018, 13, 72–79.
- 9 C. L. Long, D. P. Qi, T. Wei, J. Yan, L. L. Jiang and Z. J. Fan, *Adv. Funct. Mater.*, 2014, 24, 3953–3961.
- 10 L. L. Jiang, L. Z. Sheng, C. L. Long, T. Wei and Z. J. Fan, *Adv. Energy Mater.*, 2015, 5, 1500771.
- 11 Q. H. Zhou, J. Chang, Y. T. Jiang, T. Wei, L. Z. Sheng and Z. J. Fan, *Electrochim. Acta*, 2017, 251, 91–98.
- 12 X. L. Wu, D. R. Yang, C. K. Wang, Y. T. Jiang, T. Wei and Z. J. Fan, *Carbon*, 2015, 92, 26–30.
- 13 Q. Wang, J. Yan, Y. Xiao, T. Wei, Z. J. Fan, M. L. Zhang and X. Y. Jing, *Electrochim. Acta*, 2013, 114, 165–172.

- 14 X. Y. Deng, S. Zhu, J. J. Li, F. He, E. Z. Liu, C. N. He, C. S. Shi, Q. Y. Li, L. Y. Ma, N. Q. Zhao, *Carbon*, 2019, 143, 728–735.
- 15 G.-H. An and H. J. Ahn, *Appl. Surf. Sci.*, 2019, 473, 77–82.
- 16 H. F. Zhang, X. J. He, J. Gu, Y. Y. Xie, H. F. Shui, X. Y. Zhang, N. Xiao and J. S. Qiu, *Fuel Process. Technol.*, 2018, 175, 10–16.